

УДК 547.64

DEFINITE CHIRALITY MEASURES FROM ELECTRON TORSION: APPLICATION TO HELICAL MOLECULES

A.V. Luzanov* and M.M. Kukuiev*

The previously given pseudoscalar chirality index based on the electron path torsion [Struct. Chem. 3, 175 (1992)] is modified, and the corresponding positive definite chirality measure is proposed. The approach is applied to helicenes and DNA double-stranded minihelices. In addition, the electronic chirality measure is divided into atomic contributions. It allows to provide an appropriate pictorial presentation of molecular chirality. Several model examples of discrete helix structures are given. They offer an understanding of non-trivial differences in describing molecular chirality by aid of the pseudoscalar torsion invariants and by aid of the positive orbital torsions proposed in the present paper.

Keywords: molecular chirality, chirality operator, LCAO representation, helicenes, DNA minihelices.

Introduction

Certainly, chirality is a remarkable paradigm which embraces various sides of science and nature. In chemistry, molecular chirality was discovered by Pasteur (at age 25!). Mathematical models of the molecular chirality were proposed first by Guye after more than forty years (for detail see [1]). The problem of chirality quantification is also the old one, and for molecular structures it was discussed and carefully investigated in many works, starting from the Kitaigorodskii book [2]. Further development was discussed and overviewed in [1,3-6]).

It must be stressed that no fully acceptable solution to this problem can be achieved if we assume that both geometrical and physicochemical aspects should be taken into account. Really, from the mathematical viewpoints, the chirality measure is required to be a nonnegative function of molecular geometrical parameters. The measure must be vanishing if and only if the molecular structure is achiral [3,5,6]. At the same time, physical and physicochemical chiral systems are usually described by extensive (additive) pseudoscalar quantities, such as the angle of optical rotation or helical twisting power (in cholesteric liquid crystal mixtures). It is important that all these pseudoscalar characteristics are of electronic nature. However, they can be zero-valued even in some definitely chiral systems too. That is why pseudoscalars are not able to provide consistent chirality measurement, as it was clearly shown by Weinberg and Mislow [6]. On the other hand, we showed in [7] that the nonnegative (simply, positive) definite chirality measures cannot consistently furnish the additivity (more exactly, additive separability). The latter property guarantees vanishing of chirality measures for racemic mixtures. It seems that researchers usually remain unaware of this unsolvable dilemma. In this situation we must make a choice of the "lesser evil", that is we prefer to use more correct semi-positive chirality measures.

Indeed, specific examples (some of them are given in Ref. [8]; see also critique in Ref. [9]) tell us that the additive pseudoscalar chirality index from our first works [10,11] can be unsuitable for quantifying molecular chirality in sufficiently large systems. On this account we elaborated recently a special procedure transforming molecular pseudoscalars into positive definite quantities [12]. Unfortunately, this approach is rather laborious for very large systems because it includes many numerical integrations.

In this paper we propose a modified approach which is much simpler. Unlike most of the existing positive measures, this new index quantifies the electronic chirality rather than the geometrical or shape chirality. We implemented the appropriate procedure within the Mathematica 5.2 environment and made some illustrations for two representative classes of helical structures (helicenes and minihelices of DNA). In Appendix we consider in more detail the additivity problem of chirality measures, and provide the additional illustration on modeled helices.

* SSI "Institute of Single Crystals", NAS of Ukraine, 60 Science Ave., 61078 Kharkiv, Ukraine

Definite orbital torsions

First we recall the previously given technique of quantifying molecular chirality by the electron path torsion [7,8]. In the cited works the well-known differential-geometric notion of curve torsion is used as a starting point. The respective linear Hermitian operator of the torsion ('chirality operator'), \hat{K} , is constructed to be

$$\hat{K} = \{(\mathbf{p} \wedge \dot{\mathbf{p}} - \dot{\mathbf{p}} \wedge \mathbf{p}) \cdot \ddot{\mathbf{p}} + \text{h.c.}\} / 4, \quad (1)$$

where \mathbf{p} is the one-electron momentum operator, h.c is the Hermitian conjugation, and dots above symbols denote the time derivatives of corresponding order. Each such derivative is computed by a standard commutation of \mathbf{p} (then of $\dot{\mathbf{p}}$ etc.) with one-electron Hamiltonian, h , of the system in question. In practice, the needed matrices (instead of operators) are rather easily constructed, especially within typical semiempirical schemes of quantum chemistry.

Having at our disposal the \hat{K} matrix we can directly calculate the overall chirality measure κ_0 as follows:

$$\kappa_0 = \text{Tr } \hat{K}. \quad (2)$$

This is the basic pseudoscalar chirality index in our approach. In order to pass to definite measures we divide the index into orbital contributions. For this we introduce a full set of eigenvectors of h , in other words, an appropriate MO set $\{|\varphi_j\rangle\}$ in a conventional LCAO representation. With each $|\varphi_j\rangle$ having orbital energy ε_j , the orbital chirality index is defined to be

$$\kappa_j = \text{Tr } \hat{K} |\varphi_j\rangle \langle \varphi_j| = \langle \varphi_j | \hat{K} | \varphi_j \rangle. \quad (3)$$

Then Eq. (2) is obviously tantamount to a spectral sum of the form

$$\kappa_0 = \sum_j \kappa_j, \quad (4)$$

where the sum is over all MOs existing within the model used.

Now restrict ourselves by a class of low-symmetry molecular systems (no orbital degeneracy). In this case all MOs belong to one-dimensional irreducible representations, so all orbital projectors

$$P_j = |\varphi_j\rangle \langle \varphi_j|$$

are totally symmetric. Next, take into account that (1) is a pseudoscalar operator. Then if the system achiral, \hat{K} changes its sign under improper symmetry operations, but P_j does not. Thus, in agreement with (3) all orbital chiralities κ_j disappear, and $\kappa_0 = 0$, as it must be for achiral molecules. In chiral molecules only proper rotations are possible, and \hat{K} is invariant under these operations. So generally, indices $\kappa_j \neq 0$ but among them some κ_j are positive and some negative. Now it is clear that it is possible that in sum (4) these values are almost mutually compensated, and it may cause an incorrect measurement of the electron chirality. To avoid these situations we replace κ_j in (4) by their absolute values. Thus the new definition of the electronic chirality measure is

$$\kappa = \sum_j |\kappa_j|. \quad (5)$$

For understanding differences between this positive chirality measure and pseudoscalar index χ previously given in Ref. [10], it is worth examining chirality in simple discrete helices as done in Appendix.

The overall chirality index (5) can be partitioned into atomic contributions $\{\kappa_A\}$ as follows

$$\kappa_A = \sum_j |\kappa_j| P_j^A, \quad (6)$$

where P_j^A is the Löwdin-type population of MO $|\varphi_j\rangle$ on atom A . Eqs. (5) and (6) are basic in the proposed definite chirality scheme for the low symmetry structures. Notice that the Löwdin popula-

tions are normally based on the squared LCAO coefficients. We prefer using more localized representation which is generated by the normalized quartic (fourth power) LCAO coefficients. For modeling the electronic structure of the studied systems we used the extended Hückel method with parameters of Hoffmann [13].

In the case of high symmetry systems the above scheme is somewhat reformulated. Now, instead of individual $|\varphi_j\rangle$, we must take a whole subset of MOs related to degenerate (in general) energy level ε_j :

$$|\varphi_j\rangle \rightarrow \{|\varphi_{j,\alpha}\rangle\}_{1 \leq \alpha \leq \nu[j]},$$

where $\nu[j]$ is a multiplicity of ε_j . Then

$$P_j = \sum_{\alpha=1}^{\nu[j]} |\varphi_{j,\alpha}\rangle \langle \varphi_{j,\alpha}|$$

and

$$\kappa_j = \text{Tr } \hat{K} P_j = \sum_{\alpha=1}^{\nu[j]} \langle \varphi_{j,\alpha} | \hat{K} | \varphi_{j,\alpha} \rangle.$$

With these replacements, Eqs. (5) and (6) remain unchanged, as well as the above considered selection rules do.

To conclude this section we present the results of computations on Eqs. (5) and (6) for the D_2 symmetry conformation of cyclohexane. This twist-boat structure is a paradigmatic example in conformation analysis and molecular chirality [14,15]. In Refs. [8,12] we even used $\kappa[\text{C}_6\text{H}_{12}]$ as a suitable unit for chirality measurements. We display in Fig. 1 the plane projection of the system (so some CH and CC bonds are superimposed); here and elsewhere the green discs (carbon atoms) and black discs (hydrogen atoms) have the diameter proportional to the corresponding atomic chirality index. From Fig. (1) we see that H atoms (50% of all atoms) contribute to a small extend (in fact almost 7%). In most of the systems we studied here, such a contribution is even lesser, and we will suppress the hydrogen atoms in all subsequent chirality diagrams. It is worth mentioning that the chirality index is distributed unevenly over the carbon skeleton of cyclohexane: more preferable are two C atoms lying on the long C_2 rotation axis (see Fig. 1). Other examples (see below) support this rather general rule. In what follows we will use the mentioned cyclohexane units: $\kappa[\text{C}_6\text{H}_{12}] = 19.872$ atomic units.

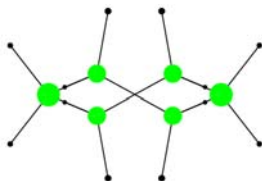


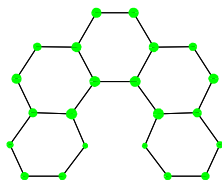
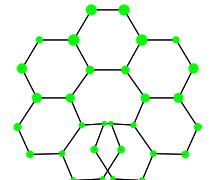
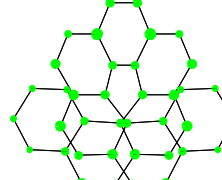
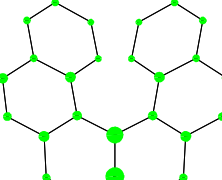
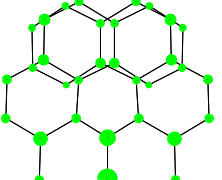
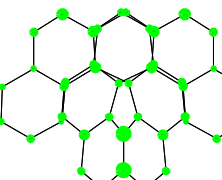
Figure 1. The chirality distribution over the cyclohexane molecule.

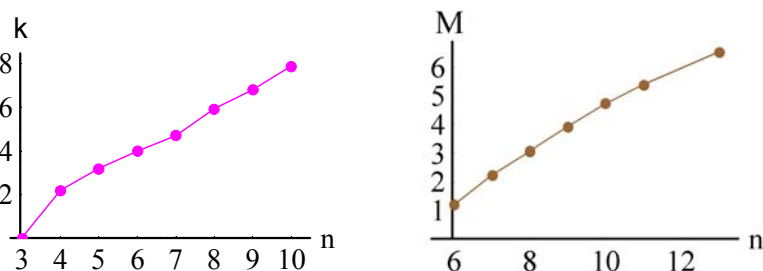
Helicenes

Helicenes belong to a very interesting class of axial chirality molecules. They have been investigated extensively in chemistry more than one hundred years [16]. The chirality quantification for helicenes was also studied [7,17,18]. Here we report the results of computing κ -index and chirality distribution $\{\kappa_A\}$ for the same systems (Table 2). We observe from the table that in the even members of $[n]$ helicenes (the last row in Table 1) the chirality is somewhat more localized than in the odd ones. In the even members the chiral (C_2) axis passes through a C-C bond whereas in the odd members it passes perpendicular to a C-C bond. Thus, the rule postulated in the above section evidently works in helicenes as well.

One more questionable point we would like to discuss concerns a size (or n) dependence of κ for helicenes. For convenience, we give in Fig. 2 relevant plots of κ and molar rotation $[M]$ (taken from [19]) against n .

Table 1. Chirality index κ and chirality distribution $\{\kappa_A\}$ in $[n]$ helicenes Table 1. Chirality index κ and chirality distribution $\{\kappa_A\}$ in $[n]$ helicenes

n	κ	$\{\kappa_A\}$	n	κ	$\{\kappa_A\}$	n	κ	$\{\kappa_A\}$
5	3.2		7	4.7		9	6.8	
6	4.0		8	5.9		10	7.9	

**Figure 2.** Size dependence of chirality (the left panel) and molar rotation $[M]$ taken from Ref. [19] (the right panel) for n [helicenes]. $[M]$ is scaled by factor 10000.

It is clear that like $[M]$, the new κ -index approximately behaves monotonically with increasing n . The similar behavior was described previously in Ref. [19]. However, somewhat another dependences were reported in Refs. [17,18] (occurrence of minimum near $n=8$ in Ref. [17] and minimum and maximum near $n=10$ in Ref. [18]). We cannot grasp these peculiarities by the usual geometric reasoning. As there are no other reported results for the same systems, this issue, raised in [7], remains unclear.

DNA minihelices

DNA minihelices are an inevitable simplification of native DNA if we are trying to understand the most important molecule of life [20] by quantum chemistry methods. Small self-complementary minihelices were studied in various theoretical aspects almost more than forty years [21]. At present, more sophisticated models of DNA examined at the DFT level can be provided [22,23], and here we will use the optimized geometry structures obtained in these works.

It is worth noting that within DNA problem the molecular chirality measures were first considered only quite recently in an extensive study of Pietropaolo and Parrinello [24]. Their work is based on the pseudoscalar chirality index introduced in [25,26] (this index is just criticized by Weinberg and Mislow [6]). Below we describe our results for DNA minihelices analyzed by the positive definite chirality measure.

We use the conventional notations, and following Refs. [22,23] we consider double-stranded $d(A)_3d(T)_3$ and $d(G)_3d(C)_3$ minihelices. The representative results are given in Tables 2 and 3. When computing individual single-stranded fragments (strands in the tables) we take the corresponding fro-

zen part of the whole duplex structure (using the same molecular geometry as in the whole system of interest). The excess, $\Delta\kappa$, is defined as the difference between the actual κ value for the whole system ('united' in Table 1) and that from the sum of κ for the frozen subsystems (strands 1 and 2 in our case). Turning to Table 2 we see that the B-form of the individual trinucleotide strands is certainly more chiral than the respective A-form. Furthermore, $d(G)_3d(C)_3$ is more chiral than $d(A)_3d(T)_3$ but only in the B-form, whereas the respective A-forms have practically the same chirality.

Notice that our index is fairly sensitive to small variations of structural molecular parameters. Nevertheless, the chirality difference between A- and B-form of the individual strands remains the same even for rather strong perturbations of the atomic coordinates. In a sense, thermal vibrations can be treated as such a perturbation. To be more specific, we give below the results of a simple simulation of structurally perturbed DNA minihelices. We introduced slight random distortions of the molecular geometry by adding a random displacement vector to every atomic coordinate (maximal variation was fixed to be 0.05 \AA). Then usual computations were performed for several such perturbed systems (a number of trials was 5), and the usual averages (denoted by $\kappa[\text{pert}]$) were obtained. In particular, we found that in strand $d(A)_3$ $\kappa[\text{pert}]$ is equal to 3.11 and 3.80 for the perturbed A- and B-forms, respectively. In other words, in this case we have no principal differences, in comparing with the data of Table 2. The analogous are results for other individual strands. Qualitatively the situation in the double minihelices is also not in sharp contrast to that of the unperturbed systems. In the case of double minihelices Ia and IIa we obtained the $\kappa[\text{pert}]$ values 5.65 and 5.60, respectively, which are not significant different. Systems Ib and IIb are a little more different: the $\kappa[\text{pert}]$ values are 7.38 and 7.28, respectively. This is a smaller difference than in Table 2, but still sufficiently marked. Surely, the above consideration is only preliminary, and more refined techniques should be elaborated to judge about significant or not significant chirality differences in various types of problems.

We also see that $\Delta\kappa$ is rather small (few percents), especially in A- $d(A)_3d(T)_3$. Hence, inter-strand nonadditivity effects, which are mainly due to long-distance interactions, can be negligible in our chirality analysis.

Table 2. Chirality index κ and excess $\Delta\kappa$ for A- and B-forms of $d(A)_3d(T)_3$ and $d(G)_3d(C)_3$ minihelices.

	minihelix	κ [strand 1]	κ [strand 2]	κ [United]	$\Delta\kappa$
Ia	A- $d(A)_3d(T)_3$	3.22	2.90	5.69	-0.18
Ib	B- $d(A)_3d(T)_3$	3.81	3.80	7.43	-0.43
IIa	A- $d(G)_3d(C)_3$	2.94	3.14	5.69	-0.39
IIb	B- $d(G)_3d(C)_3$	3.92	3.65	7.26	-0.31

Table 3. Summary chirality indices (in %) $\kappa[C]$, $\kappa[N]$, $\kappa[O]$, $\kappa[P]$, and $\kappa[H]$ related to the corresponding atoms of individual frozen strands in A- and B-forms of the duplexes

Strand	$\kappa[C]$	$\kappa[N]$	$\kappa[O]$	$\kappa[P]$	$\kappa[H]$
A- $d(A)_3$	38	27	28	2	6
B- $d(A)_3$	50	18	24	2	6
A- $d(T)_3$	45	11	35	4	6
B- $d(T)_3$	54	8	32	2	5
A- $d(G)_3$	38	23	31	3	6
B- $d(G)_3$	50	16	26	2	5
A- $d(C)_3$	42	11	37	3	7
B- $d(C)_3$	54	6	31	2	6

Now we will try to understand one interesting point concerning the extent to which the chirality in DNA strands owes to the dissymmetric sugar-phosphate backbone, and what is the role of the nitrous bases. To this end we denote by SP the sugar phosphate backbone (consisting of 5-carbon deoxyribose sugars and phosphate groups), and define $\kappa[\text{SP}]$ as the sum of κ_A over all SP atoms. As a result,

we find that only slightly more than 50% of the total κ value is reproduced by such ‘base-free’ sugar-phosphate backbone subsystem. For instance, in B-d(A)₃ we obtain $\kappa[\text{SP}] / \kappa = 0.53$. This behavior of κ is not in the same line with the results of work [24]. In the latter the sugar-phosphate fragments (more exactly, only very short segments of polynucleotide strings) are considered when quantifying DNA chirality by the pseudoscalar index. The rest of the DNA molecule was ignored in [24]. However, the molecular chirality is a too complicated property for simple interpretation in terms of only local regions and related notions. That is why the examination of the whole system, not its small parts only, is desirable from the very beginning. The data of Table 3 where we display the summary contributions from all types of atoms (C, N, O, P, and H), are also in agreement with this viewpoint. In this table we see that for the minihelices the next-most important (after carbon atoms) are oxygen atoms. Even the phosphorus atoms give relatively small contribution to the overall chirality. The additional insight is provided by atomic distributions $\{\kappa_A\}$. We will exhibit only two relevant examples of the strands taken from B- d(A)₃d(T)₃ (see Fig. 3).

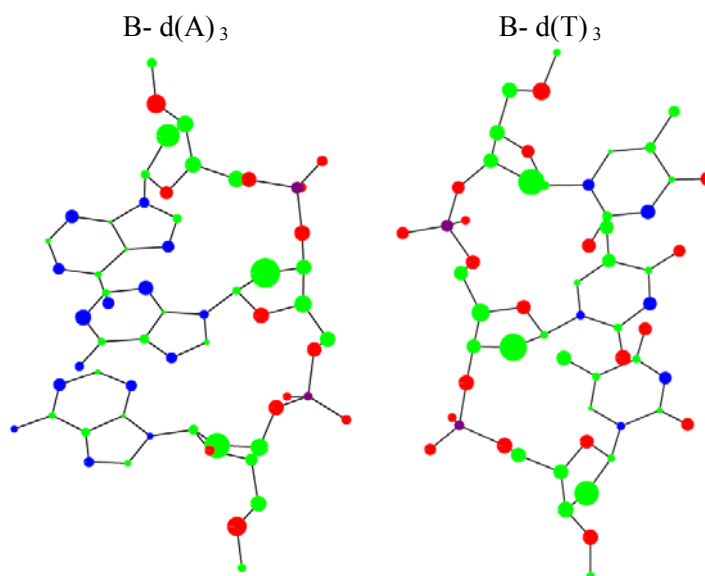


Figure 3. The atomic $\{\kappa_A\}$ distribution for the frozen B- d(A)₃ and B- d(T)₃ structures. The nitrogen atoms are highlighted in blue, oxygen atoms in red, and four-coordinate phosphorus atoms in magenta.

Conclusion

In the present paper we proposed the new chirality quantification scheme based on modifying previous works [7,10]. Essentially, we were able to preserve the differential-geometry background of the whole approach and produce here the positive definite chirality measure. With help of this it is simple to examine the electronic chirality in large systems such as DNA-like structures. Furthermore, the atomic decomposition of the overall chirality measure is defined, and a visual chirality portrait of molecule can be easily made. At least, It is also interesting to understand the chirality in simple discret-type model helices as done in Appendix.

In most of the examples considered here we observed a sufficiently delocalized picture of the distributed chirality. Specifically, a significant contribution of the nitrous bases in the DNA minihelices is obtained. This feature is not so unusual if we recall the approximate analysis of local atomic contributions to the optical rotation given recently in Refs. [27,28]. In the cited works it was shown that even “the chemical groups far from stereogenic centers can dominate the chiroptical effects” [27]. Indeed, there is a general effect of inducing optical activity in achiral molecules or achiral fragments which interact with dissymmetric molecular subunits. This effect was interpreted long ago for the polynucleotides in which the circular dichroism in the nitrous bases arises mainly from $\pi\pi^*$ - transitions [29]. It is desirable to continue the presented studies, and involve in future more sophisticated techniques. However, the main inference from the above results about a global chiral structure of helical networks seems reasonable and, we believe, will be stable with respect to the more extended techniques.

Acknowledgment

The authors are grateful to L. G. Gorb and T. A. Zubatiuk for giving us the optimized geometry structures of the DNA minihelices and for valuable discussions on the related problems. Furthermore, we thank the unknown referee for important points brought to our attention.

Appendix

Here we additionally discuss the peculiarities of the proposed chirality measure. First, we repeat the argumentation from Ref. [7] about the incompatibility of positivity and additivity requirements for chirality measure. The proof is almost trivial. Let the given chirality index χ be an additive measure. Then for two isolated species A and B we have $\chi(A+B) = \chi(A) + \chi(B)$. Now take B as a mirror image of A , and signify the latter by $A^\#$. From the above additivity requirement we have $\chi(A+A^\#) = \chi(A) + \chi(A^\#)$. But the united system $A+A^\#$ comprising of the isolated A and $A^\#$ is generally considered as achiral ('racemate') what means $\chi(A+A^\#) = 0$. Thus, $\chi(A) = -\chi(A^\#)$ for the additive χ , and this property satisfies by all existing pseudoscalar index. At the same time, the opposite identity $\kappa(A) = \kappa(A^\#)$ is valid for any positive chirality measure κ . Notice that pseudoscalar index from Ref. [25] remains in use (see, e. g., review [30]), despite the strong critique Weinberg and Mislow have given in Ref. [6].

This contradiction can be demonstrated for the model helix-like structures which we studied previously in Ref. [10] within the pseudoscalar approach. Now we present the extended study which can clarify the above analysis. Namely we will use a finite set of atoms lying in a discrete circular helix of the form:

$$x_j = \cos t_j, \quad y_j = \sin t_j, \quad z_j = a t_j,$$

where $t_j = 2\pi j / m$, and $j = 0, \dots, (m-1)\nu$. Here a is a helix pitch parameter; m is a number of atoms in each turn, and ν is a number of turns. For the specific calculations given in Table 4 we used $m = 6$ and $\nu = 5$ to produce a basic helix (structure I in the table). The next system II is the same I with an opposite twist (more exactly, opposite handedness). The identical helices with the same handedness are linked in [I,I] and in [I,II] two helices with opposite handedness are asymmetrically united. At last, in the racemic structure I+II, helices I and II are not linked. Notice that there exists a fine distinction between handedness and chirality ("All handed objects are chiral, but not all chiral objects are handed" [31]).



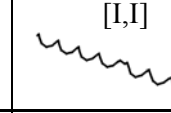
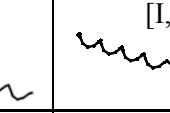

We computed the above described systems within the topological model [10] which employs a Hückel-type Hamiltonian h for Eq. (1). In Table 4 we can see all the expected differences in behavior of two kinds of the considered chirality measures. In particular, in the linked structure [I,II] the local chiralities are almost compensated, and both indices predict a slightly chiral structure. At the same time, for racemic mixture I+II, only the positive measure κ detects an occurrence of local chiral structures, but pseudoscalar measure χ and most physical and physicochemical observations do not. It is worth turning attention to equal values of $|\chi|$ and κ for the first three systems in Table 4. This fact is owing to a specific simplicity of discrete helices and their orbital properties. Of course, generally, $|\chi| \neq \kappa$, and significant differences between these measures occur too frequently.

The above results can be generalized to an arbitrary system $A+B+\dots+C$ of non-interacting subunits. If these subunits are randomly situated in a real space ("in general position"), then

$$\kappa[A+B+\dots+C] = \kappa[A] + \kappa[B] + \dots + \kappa[C].$$

Strictly speaking, this is not the additivity law, because the individual subunits can have different handednesses, and the above expression does not reflect this possibility. If cluster $A+B+\dots+C$ is achiral in toto (that is the cluster is not in general position), then automatically $\kappa = 0$.

Table 4. The pseudoscalar chirality measure χ and positive measure κ for various model helices.All quantities are given in units of κ -value for one helix turn (6 atoms).

					
χ	-7.667	7.667	-16.637	0.318	0.
κ	7.667	7.667	16.637	0.319	15.333

References

1. M. Petitjean, *Entropy* 5, 271 (2003).
2. A. I. Kitaigorodskii, *Organic Chemical Crystallography* (Consultans Bureau Ets. Inc., New York, 1961).
3. D. Avnir and H. Zabrodsky, P. G. Mezey, in *Encyclopedia of Computational Chemistry*, edited by P. v. R. Schleyer (Wiley, Chichester, 1998), vol. 4, p. 2890.
4. K. Mislow, *Top. Stereochem.* 22, 1 (1999).
5. G. Gilat, *J. Math. Chem.* 15: 197(1994).
6. N. Weinberg and K. Mislow, *Can. J. Chem.* 78, 41(2000); G. Millar, N. Weinberg, and K. Mislow, *Mol. Phys.* 103, 2769 (2005).
7. A. V. Luzanov and D. Nerukh, *J. Math. Chem.* 41, 417 (2007).
8. A V. Luzanov, *Int. J. Quantum Chem.* 111, 2196 (2011).
9. R. Natarajan and S. C. Basak, *Current Computer-Aided Drug Design* 5, 13 (2009).
10. A. V. Luzanov and E. N. Babich, *Struct. Chem.* 3, 175 (1992); A. V. Luzanov and E. N. Babich, *Theochem.* 333, 279 (1995).
11. A. V. Luzanov, V. V. Ivanov, and R. M. Minyaev, *J. Struct. Chem.* 39, 261 (1998).
12. A. V. Luzanov, *Funct. Mater.* 22, 355 (2015).
13. R. Hoffmann, *J. Chem. Phys.* 39, 1397 (1963); <http://www.quantumwise.com/documents/manuals/ATK-2014/ReferenceManual/index.html/chap.atomicdata.html#sect3.atomicdata.huckel.hoffmann>.
14. V. I. Sokolov, *Introduction to theoretical stereochemistry* (Gordon and Breach, New York, 1991).
15. D. J. Nelson and C. N. Brammer, *J. Chem. Ed.* 88, 292 (2011).
16. M. Gingras, *Chem. Soc. Rev.* 42, 968 (2013).
17. S. Grimme, *Chem. Phys. Lett.* 297, 15 (1998).
18. O. Katzenelson, J. Edelstein, and D. Avnir, *Tetrahedron Asymmetry* 11, 2695 (2000)].
19. H. Laarhoven and J. C. Prinsen, *Top. Curr. Chem.* 125, 63 (1984).
20. M. D. Frank-Kamenetski, *Unraveling DNA. The most important molecule of life* (Addison-Wesley, New York, 1997).
21. A. Pullman, C. Zakrewska, and D. Perahia, *Int. J. Quantum Chem.* 16, 395 (1979); D. Perahia and A. Pullman, *Theor. Chim. Acta* 50, 351 (1979).
22. T. A. Zubatiuk, O. V. Shishkin, L. Gorb, D. M. Hovorun, and J. Leszczynski, *Phys. Chem. Chem. Phys.* 15, 18155 (2013).
23. T. A. Zubatiuk, M. A. Kukuiev, A. S. Korolyova, L. Gorb, A. Nyporko, D. Hovorun, and J. Leszczynski, *J. Phys. Chem. B* 119, 12741 (2015).
24. A. Pietropaolo and M. Parrinello, *Chirality* 23, 534 (2011).
25. M. A. Osipov, B. T. Pickup, and D. A. Dunmur, *Mol. Phys.* 84, 1193(1995).
26. M. Solymosi, R. J. Low, M. Grayson, and M. P. Neal, *J. Chem. Phys.* 116, 9875 (2002).
27. R. K. Kondru, P. Wipf, and D. N. Beratan, *Science* 282, 2247 (1998); R. K. Kondru, P. Wipf, D. N. Beratan, G. K. Friestad, and A. B. Smith, *Org. Lett.* 2, 1509 (2000).
28. P. Mukhopadhyay, P. Wipf, and D. N. Beratan, *Acc. Chem. Res.* 42, 809 (2009).
29. W. C. Johnson, I. Tinoco, *Biopolymers* 7, 727(1969).
30. A. Pietropaolo, in: *Ideas in Chemistry and Molecular Sciences: Where Chemistry Meets Life*, ed. B. Pignataro. (Wiley-VCH, Weinheim, 2010), p. 293-311.
31. R.B. King, *Ann N Y Acad Sci.* 988, 158 (2003).

Поступила до редакції 1 вересня 2016 р.

А.В. Лузанов, М.А. Кукуев. Дефинитная мера хиральности из электронного кручения: применение к спиральным молекулам.

Модифицирован предложенный ранее псевдоскалярный индекс хиральности, основанный на кручении электронных траекторий, и предложена положительно определенная мера хиральности. Подход применен к гелиценам и двойным миниспиральям ДНК. В дополнение, электронный индекс разбивается на атомные вклады, что позволяет дать наглядное графическое представление молекулярной хиральности. Представлено несколько модельных примеров дискретных спиральных структур. Они дают понимание нетривиального различия в описании молекулярной хиральности с помощью псевдоскалярного инварианта кручения и с помощью положительных орбитальных кручений, предложенных в данной статье.

Ключевые слова: молекулярная хиральность, оператор хиральности, представление ЛКАО, гелицены, миниспирали ДНК.

А.В. Лузанов, М.А. Кукуев. Дефинітна міра хіральності з електронного скруту: застосування до спіральних молекул.

Модифіковано раніше введений псевдоскалярний індекс хіральності, що був заснований на скруті електронних траєкторій, та запропоновано позитивно визначену міру хіральності. Підхід застосовано до геліценів та подвійних мініспіралей ДНК. Додатково електронний індекс розкладається на атомні внески, що дозволяє наочне графічне представлення молекулярної хіральності. Розглянуто декілька модельних прикладів дискретних спіральних структур. Вони допускають тлумачення нетривіальної різниці в описуванні молекулярної хіральності за допомогою псевдоскалярного інваріанта скруту та за допомогою позитивних орбітальних скрутів, що запропоновані в даній роботі.

Ключові слова: молекулярна хіральність, оператор хіральності, представлення ЛКАО, геліцени, мініспіралі ДНК.

Kharkov University Bulletin. Chemical Series. Issue 27 (50), 2016